Redox-induced Catalysis

3MEH.DE

$$R^1-NH_2 + \equiv\!\!-R^2 \xrightarrow[\text{d}_6\text{-benzene}]{\substack{\text{[FeAu] red./ox. (cat.)}\\ \text{NaBAr}^F}} \begin{array}{c} R^1 \\ N \\ \parallel \\ H_3C \quad R^2 \end{array}$$

[FeAu] ox.

[FeAu] red.

x-axis: time [h] (0, 5, 10, 15, 20, 25)
y-axis: $1/c$ [M^{-1}] (0, 10, 20, 30, 40)

DOWN TO 0.001 MOL%

Me / Me / Me / Me / Me / Me
Fe
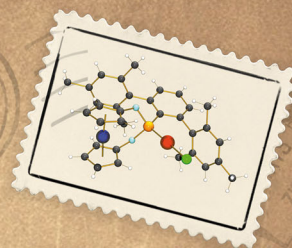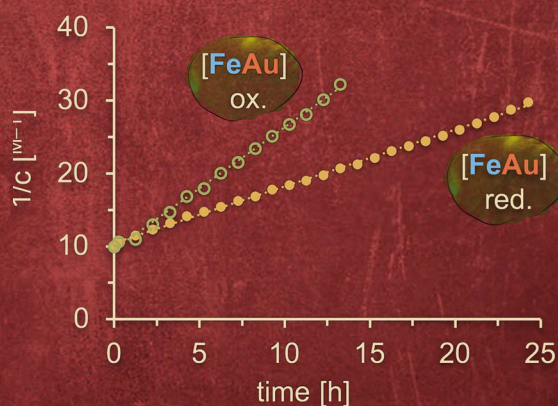P
O O
Au
Cl

Showcasing research from the groups of Jan Paradies from the University of Paderborn and Frank Breher from the Karlsruhe Institute of Technology (KIT).

Redox-responsive phosphonite gold complexes in hydroamination catalysis

Very high activities were observed in the redox-induced hydroamination of alkynes by employing a redox-active gold(I) complex featuring a phosphonite-based ligand. Very low catalyst loadings (down to 10 ppm) and very mild conditions (25 °C) were used.

As featured in:

ChemComm
Chemical Communications

See Jan Paradies, Frank Breher *et al.*, *Chem. Commun.*, 2019, **55**, 5323.

ROYAL SOCIETY OF CHEMISTRY | Celebrating IYPT 2019

rsc.li/chemcomm

COMMUNICATION

Check for updates

Redox-responsive phosphonite gold complexes in hydroamination catalysis†

Eva Deck,[a] Hanna E. Wagner,[a] Jan Paradies [ID] *[b] and Frank Breher [ID] *[a]

Very high activities were observed in the redox-induced hydroamination of alkynes by employing a redox-active gold(ı) complex featuring an electron-deficient, terphenyl-substituted phosphonite-based ligand. The hydroamination proceeds roughly two-fold faster with the *in situ* oxidized catalysts than with their reduced form.

Tertiary phosphines (PR$_3$) and phosphites (P{OR}$_3$) represent some of the most important classes of ligands in transition metal chemistry and their steric and electronic properties can be easily adjusted.[1] Although many variations of P-donor ligands have been described in the past, the development of new phosphines with exceptional donor[2–4] or acceptor[5] capacities or steric properties[6] remain in the focus of current research activities. The driving force most often originates from the unsatisfied demand to modify and adjust the properties of phosphine metal complexes, *e.g.* to face activity, selectivity, or stability issues in the field of homogeneous catalysis. Landmark examples include, for instance, the well-known biaryl phosphines developed by Buchwald and co-workers (**I**, Chart 1), which found ubiquitous applications in homogeneous catalysis.[6] One of the most important structural features of these ligands is the weak – for catalyst stability nonetheless crucial – arene π-interactions with the metal centre. In recent years, elegant variations of Buchwald-type biaryl phosphines have been reported by various groups.[7–10] Our group could recently show that the biaryl structural motif can also be included in redox-active phosphine ligands, in our case [1]phosphaferrocenophanes (**II**, Chart 1).[11] Palladium complexes thereof have been successfully applied in redox-induced[12] Buchwald–Hartwig amination reactions. Furthermore, we have successfully applied these types of ligands in redox-induced rhodium-catalysed hydrosilylation reactions and found that it is possible to alter the activity and selectivity of the catalyst by using a stimulus-responsive phosphine ligand.[13,14] Inspired by the recent developments in homogeneous gold(ı) catalysis,[15] in particular in catalytic hydroaminations,[16] we became interested in studying redox-responsive P-donor ligands in this area.

Gold-catalysed hydroamination reactions have been intensively studied in recent years. Xu and co-workers provided a comprehensive study on the influence of steric and electronic effects of phosphine ligands in the three major stages of the catalytic cycle in gold catalysis, also including catalytic hydroaminations of alkynes.[17] The first stage consists of the initial electrophilic activation of the unsaturated bond, which appears to be favoured by electron-poor ligands. In contrast, the so-called protodeauration in the second stage of the catalytic cycle is accelerated by electron-rich ligands. Although the factors influencing the catalyst deactivation are more complex, biaryl-decorated phosphine ligands were found to be beneficial in terms of catalyst stability. To this end, a very active gold(ı) complex (**III**, Chart 1)[18] has been recently presented showing high efficiency at very low loadings (25 ppm) and relatively low temperatures (50 °C) in the gold-catalysed intermolecular hydroamination of alkynes. It is commonly accepted that for this type of catalysis, the protodeauration step[19] is rate-determining, which should – in principle – be even more accelerated by increasing the donor-strength of the ligands. However, exceptions from this rather simple recipe have also been observed, such that most electron-rich phosphines are not
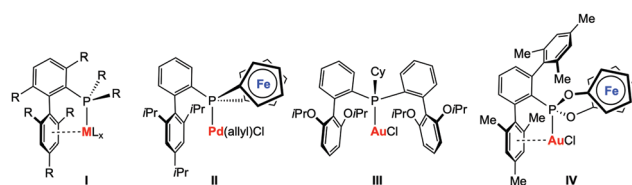

Chart 1 Selected metal complexes with Buchwald-type ligand architectures (**I–III**) from the literature; target structure **IV** of this study.

[a] *Institute of Inorganic Chemistry, Karlsruhe Institute of Technology (KIT), Engesserstr. 15, 76131 Karlsruhe, Germany. E-mail: breher@kit.edu*

[b] *Department of Chemistry, University of Paderborn, Warburger Str. 100, 33098 Paderborn, Germany. E-mail: jan.paradies@uni-paderborn.de*

† Electronic supplementary information (ESI) available: Experimental details, NMR data, cyclic voltammetry data, and X-ray crystal structure data. CCDC 1898143–1898147. For ESI and crystallographic data in CIF or other electronic format see DOI: 10.1039/c9cc01492f

very efficient in triggering the hydroamination reaction.[20] We therefore became interested in studying electron-poor ligands in gold-catalysed hydroamination reactions and in elucidating the influence of a redox-switch on the catalyst performance. Based on our previous experiences in redox-switchable/-induced catalysis and our general interest in cooperative effects in multi-metallic complexes,[21] we targeted the ferrocene-based phosphonite ligand **IV** featuring both a redox-switchable entity and a Buchwald-type ligand architecture (Chart 1).

Although aryl- and alkyl-substituted 1,3-dioxa-2-phospha-[3]-ferrocenophanes have already been described before by Herberhold and co-workers,[22] their coordination chemistry or further substitution of the P-bound ligand has not been reported so far. The ligands of interest (**1**: R = Ter = 2,6-Mes$_2$C$_6$H$_3$; **2**: R = Ph;[22] **3**: R = tBu[22]) were synthesised according to (or by adapting) the literature protocol from 1,1'-ferrocenediol and RPCl$_2$ and obtained as orange crystals after work-up (ESI†). The ligands were fully characterised, also including the molecular structures of **1** and **3** (Fig. 1). The gold(ɪ) complexes **4–6** were prepared in good yields (65–69%) by treating **1–3** with [Au(tht)Cl] in thf (Scheme 1). The successful coordination of the ligands was verified by ^{31}P NMR spectroscopy. All ^{31}P NMR chemical shifts show the expected upfield shift of *ca.* $\Delta\delta_{31P}$ = 32–34 ppm upon κ^1P-coordination (*e.g.* δ_{31P} (**1**) = 183.8 ppm and δ_{31P} (**4**) = 147.8 ppm). The structures of the complexes were determined by X-ray diffraction of suitable single crystals and confirmed the identities of the products (Fig. 1). All gold complexes display the expected linear coordination and typical Au–P bond lengths of $\sim$221 pm. The intermetallic distances between the Fe and the Au atoms vary from d(Fe$\cdots$Au) = 418.6(1) pm in **4** to 423.1(1) in **5** and 426.4(1) pm in **6**, respectively. As discussed above, low-coordinate gold complexes with Buchwald-type ligands show arene π-interactions.[23] Also in our case, short Au$\cdots$C$_{aryl}$ contacts of the gold atoms to one
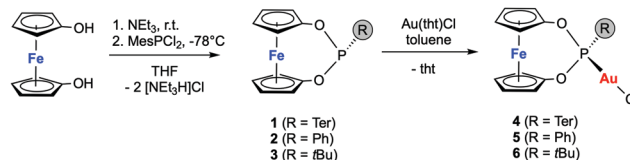
Scheme 1 Synthesis of **1–6**.

mesityl group of the terphenyl substituent were identified for **4** (d(Au1$\cdots$C115) = 308.0(5) pm and d(Au1–C116) = 313.5(6) pm; $\sphericalangle$(dihedral angle) C100–C105–C115–C116 = 86.42°), which are shorter than typically found for gold(ɪ) complexes of biaryl phosphonites.[23] Hence, a stronger stabilising effect during catalysis may be anticipated. To determine the steric demand of the studied [3]ferrocenophanes **1**, **2** and **3**, their buried volumes (%V_{bur})[24] were calculated using the crystal structure data of the gold complexes and a fixed d(P–Au) of 228.0 pm. As expected, the terphenyl substituted ligand **1** (50.9%) is relatively bulky and similar to the known JohnPhos ligand (also 50.9%). For **2** and **3**, %V_{bur} values of 34.8% and 33.8%, respectively, were calculated. Although we have also determined the Tolman electronic parameter (TEP) for **1** (2063.0 cm^{-1}) from its iridium(ɪ) complex [(κ^1P-**1**)Ir(CO)$_2$Cl],[25] we refrain from a further discussion due to known problems in categorising phosphite-type ligands with TEP values.[26]

The electrochemical properties of all title compounds (**1–6**) were probed with the aid of cyclic voltammetry (Fig. S3-1/2 and Table S3-1, ESI†). The $E_{1/2}^0$ values for the (quasi)reversible iron-centred oxidations (ΔE_p = 0.12–0.21 V; i_{pc}/i_{pa} = 1) depend on the coordinated transition metal fragment. Large anodic shifts of the iron-centred redox events are observed when the pure ligands (*e.g.* **1**: $E_{1/2}^0$ = 0.03 V) are compared with their gold complex (*e.g.* **4**: $E_{1/2}^0$ = 0.30 V). In line with our previous studies,[11,13] this trend provides indications for a good electronic communication between the metal atoms, although slightly weaker than in the [1]ferrocenophane complexes reported earlier by our group.[11,13] Nevertheless, it should be possible to alter the electronic properties of the gold(ɪ) atom by simply changing the oxidation state of the ferrocene unit. The results prompted us to apply the stimulus-responsive metal complexes in redox-induced catalysis.

The application of complexes featuring [n]metallocenophanes as ligands in redox-switchable/-induced catalysis is limited to only some reports.[11,13,27] In gold(ɪ) catalysis, redox-responsive carbene complexes have been successfully applied by the groups of Sarkar,[28] Peris[29a] and, more recently, Heinze.[29b] In order to investigate the applicability of the bimetallic complexes reported herein, we have studied the hydroamination of terminal alkynes using **4–6** and *in situ* generated **4$^+$–6$^+$**[30] as catalysts. All reactions were performed in C$_6$D$_6$ at room temperature with NaBAr^F as a chloride scavenger and were monitored by ^{1}H NMR spectroscopy (referenced to an internal standard).

The Au(ɪ) catalysts **4–6** were evaluated in the hydroamination of terminal and internal alkynes using primary amines as nucleophiles.[31] First, we investigated the addition of aniline (**7a**) to phenylacetylene (**8a**) in the presence of 0.1 mol% gold catalyst in either the reduced or oxidized form (see Fig. 2a–c).
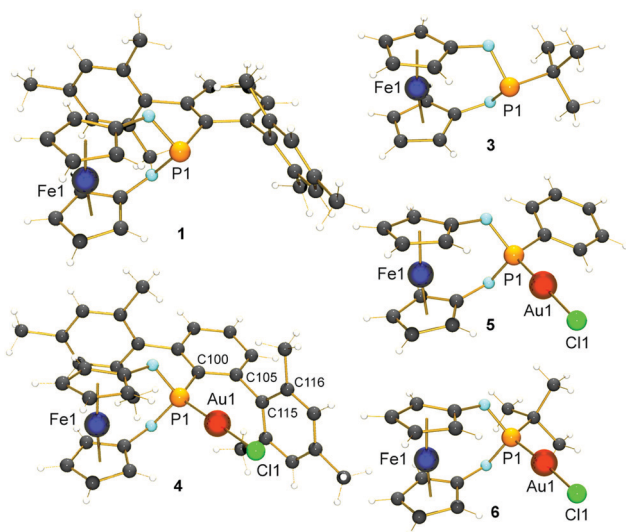

Fig. 1 Molecular structures of **1** and **3–6**. Selected distances (pm) and angles (°): **1**: Fe1$\cdots$P1 337.6(2); **3**: Fe1$\cdots$P1 330.8(1); **4**: Fe1$\cdots$P1 339.4(1), Fe1$\cdots$Au1 418.6(1), P1–Au1 220.7(1), C100–C105–C115–C116 86.42; **5**: Fe1$\cdots$Au1 423.1(1), P1–Au1 220.3(1); and **6**: Fe1$\cdots$P1 338.4(2), Fe1$\cdots$Au1 426.4(1), P1–Au1 221.4(1).
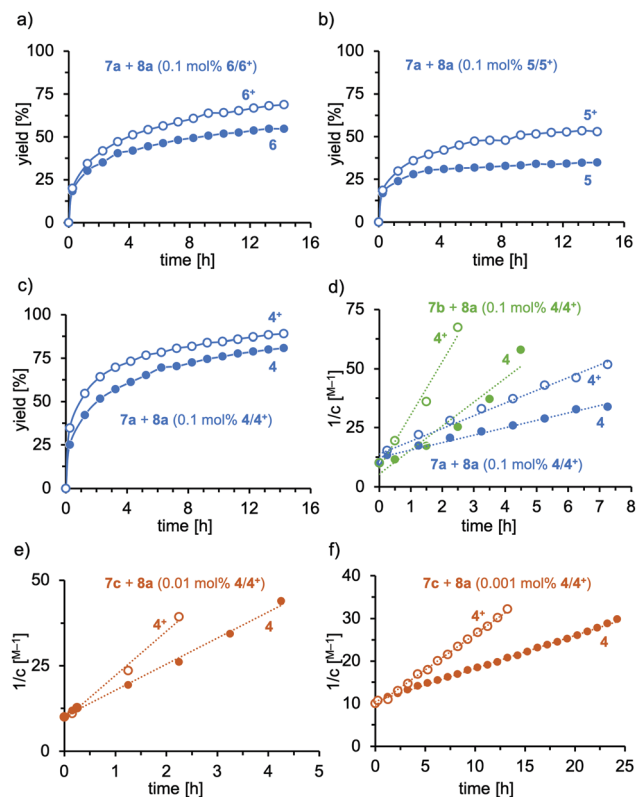
Fig. 2 (a–c) Reaction profiles of the gold-catalyzed addition of aniline (**7a**, 1.1 equiv.) to phenylacetylene (**8a**, 1.0 equiv.) using 0.1 mol% of (a) **6/6$^+$**, (b) **5/5$^+$** and (c) **4/4$^+$** at room temperature (25 °C) in C_6D_6; (d) kinetic analysis and second order rate constants of the gold-catalyzed hydroamination (0.1 mol%) of phenylacetylene (**8a**) with Ph-NH$_2$ (**7a**, blue): $k_{red\text{-}7a}$ = 3.2 M^{-1} h^{-1}; $k_{ox\text{-}7a}$ = 5.4 M^{-1} h^{-1} and Dipp-NH$_2$ (**7b**, green): $k_{red\text{-}7b}$ = 10.2 M^{-1} h^{-1}; $k_{ox\text{-}7a}$ = 22.5 M^{-1} h^{-1}; solid circles: **4**, open circles: **4$^+$**; (e) hydroamination with Mes-NH$_2$ (**7c**); 0.01 mol% **4** ($k_{red\text{-}7c}$ = 7.7 M^{-1} h^{-1}) and **4$^+$** ($k_{ox\text{-}7c}$ = 12.9 M^{-1} h^{-1}); (f) hydroamination with Mes-NH$_2$ (**7c**), 0.001 mol% **4** ($k_{red\text{-}7c}$ = 0.8 M^{-1} h^{-1}) and **4$^+$** ($k_{ox\text{-}7c}$ = 1.7 M^{-1} h^{-1}). Control reactions without any Au complex but a pure oxidation reagent gave zero hydroamination.

The *t*Bu-substituted complex **6** displayed medium activity in the hydroamination, nevertheless significant efficiency differences between the reduced and the oxidized form are apparent. The corresponding phenyl-derivative **5** was inferior to **6** and the reaction did not yield higher conversion than 50% (Fig. 2b), most probably a result of catalyst decomposition. Again, the oxidized form displayed higher activity than the reduced form. As a third system, we tested the terphenyl-substituted derivative **4** (Fig. 2c). This system displayed remarkable activity in the reduced and oxidized forms, giving 80% and 88% conversion, respectively, after 16 h at room temperature (25 °C). Notably, the reaction profiles of these catalytic reactions did not display catalyst degradation, as indicated by the second order rate plot up to 88% conversion (see Fig. S5-1, ESI†). The short Au-Mes contact, identified in the solid-state structure, has a stabilizing effect on the catalytically active cationic gold complex, which explains the poor performance of **5** and **6** in the hydroamination.

Also, the more sterically encumbered 2,6-diisopropylphenyl-amine (Dipp-NH$_2$, **7b**, green) was active in the gold-catalyzed hydroamination. Kinetic analysis of the Ph-NH$_2$ and Dipp-NH$_2$

addition to the alkyne **2a** displayed second order behavior, suggesting the nucleophilic attack of the amine as the rate-determining step (see Fig. 2d). The hydroamination proceeds roughly two-fold faster with the oxidized catalyst **4$^+$** than with its reduced form (**4**) for both amines ($k_{ox\text{-}7a}/k_{red\text{-}7a}$ = 1.7; $k_{ox\text{-}7b}/k_{red\text{-}7b}$ = 2.2). However, the hydroamination of **8a** proceeds significantly faster with Dipp-NH$_2$ (**7b**, green) than with aniline (**7a**, blue), probably as a result of the increased nucleophilicity. This picture is supported by the substantial rate increase of the hydroamination when Mes-NH$_2$ (**7c**, red) was used as a nucleophile. In fact, the reaction became too fast to obtain reliable kinetic data and the catalyst loading needed to be reduced to 0.01 mol% and 0.001 mol% (Fig. 2e and f). The catalyst shows high stability under both conditions up to high conversions. Also for this reaction, app. two-fold rate increase was observed (0.01 mol% **4**: $k_{ox\text{-}7c}/k_{red\text{-}7c}$ = 1.7; 0.001 mol% **4**: $k_{ox\text{-}7b}/k_{red\text{-}7b}$ = 2.1). The turnover frequencies for this catalytic reaction at room temperature are 784 mmol s^{-1} and 1857 mmol s^{-1} for **4** and **4$^+$**, respectively. Thereby, impressive turnover numbers (TON) of 66.000 (**4**) and 82.000 (**4$^+$**) were obtained in *ca.* 24 h at room temperature. It is important to note that only a few catalysts exist that allow for TON higher than 5.000 for the hydroamination of terminal alkynes. Lavallo and co-workers reported gold(I) complexes of a very bulky phosphine and obtained after 24 h a similar TON value of 67.000 at 10 ppm catalyst loading for the hydroamination of PhC≡CH (**8a**) with Mes-NH$_2$ (**7c**), albeit at 50 °C.[32] In our case, the reactions are performed at room temperature; furthermore, the TON can significantly be increased by *in situ* oxidation of catalyst **4**.

These kinetic data strongly support the nucleophilic addition of the amine to the activated triple bond as the rate-determining step in these phosphinate ester-derived Au catalysts in contrast to the unimolecular protodeauration of electron-rich phosphine-derived Au catalysts.

Furthermore, the catalyst system **4** was employed in the hydroamination of electron-rich, electron-deficient and aliphatic alkynes (Scheme 2). The electronic nature of the alkyne has a significant impact on the efficiency. Electron-donating groups (compare **9c** and **9g**) slowed the reaction down, which supports the notion of the nucleophilic attack being the rate-determining step. Nevertheless, all reactions went to full conversion within 24–9 hours. However, when a strongly electron-deficient alkyne is applied, the reaction becomes unproductive. The fluorinated imine **9d** is only formed in trace amounts (7%) as a result of inefficient alkyne activation by the catalyst, irrespective of the oxidation state of the iron. Aliphatic alkynes were only reluctantly hydroaminated within 24 h in medium yields. The hydroamination reactions were generally faster or gave higher yields when **4$^+$** was applied, which gives rise to externally stimulated catalyst modification. Overall, we observed high activities and impressively high TON by employing a redox-active gold(I) complex featuring an electron-deficient phosphonite-based ligand with Buchwald-type architecture in the redox-induced hydroamination catalysis of alkynes. Very low catalyst loadings (down to 10 ppm) and very mild conditions (room temperature) were used. Second order rate kinetics were observed for the addition to phenyl acetylene,

Scheme 2   Hydroamination of alkynes. Yields are given for **4** (upper value) and **4⁺** (lower value); numbers in parentheses correspond to reaction times in [h]. Reactions were conducted on a 0.1 mmol scale in d_6-benzene with 0.1 mol% **4** and 0.1 mol% NaBArF as activating agents. **4⁺** was generated *in situ* prior to the reaction by addition of 0.1 mol% [Fc(OAc)][Al{OC(CF₃)₃}₄]. The yields were determined using 1,3,5-(MeO)₃C₆H₃ as an internal standard; [a] reactions were conducted using a 1 mol% catalyst/activator.

suggesting the nucleophilic attack of the amine as the rate-determining step for this catalyst system. In these studies, the hydroamination with the three amines **7a–c** proceeds 1.7 to 2.1 times faster with the *in situ* oxidized catalysts than with their reduced form.

Conflicts of interest

There are no conflicts to declare.

Notes and references

1   J. Hartwig, *Organotransition Metal Chemistry, From bonding to catalysis*, University Science Books, Sausalito, California, 2010.
2   M. A. Wünsche, P. Mehlmann, T. Witteler, F. Buß, P. Rathmann and F. Dielmann, *Angew. Chem., Int. Ed.*, 2015, **54**, 11857.
3   T. Scherpf, C. Schwarz, L. T. Scharf, J.-A. Zur, A. Helbig and V. H. Gessner, *Angew. Chem., Int. Ed.*, 2018, **57**, 12859.
4   L. Chen, P. Ren and B. P. Carrow, *J. Am. Chem. Soc.*, 2016, **138**, 6392.
5   (a) O. René and K. Fagnou, *Adv. Synth. Catal.*, 2010, **352**, 2116; (b) P. H. Lee, S. Kim, A. Park, B. C. Chary and S. Kim, *Angew. Chem., Int. Ed.*, 2010, **49**, 6806; (c) T. Korenaga, A. Ko, K. Uotani, Y. Tanaka and T. Sakai, *Angew. Chem., Int. Ed.*, 2011, **50**, 10703.
6   (a) D. S. Surry and S. L. Buchwald, *Angew. Chem., Int. Ed.*, 2008, **47**, 6338; (b) P. Ruiz-Castillo and S. L. Buchwald, *Chem. Rev.*, 2016, **116**, 12564; (c) O. Diebolt, G. C. Fortman, H. Clavier, A. M. Z. Slawin, E. C. Escudero-Adan, J. Benet-Buchholz and S. P. Nolan, *Organometallics*, 2011, **30**, 1668.
7   Y. Wang, Z. Wang, Y. Li, G. Wu, Z. Cao and L. Zhang, *Nat. Commun.*, 2014, **5**, 3470.
8   X. Qiu, M. Wang, Y. Zhao and Z. Shi, *Angew. Chem., Int. Ed.*, 2017, **56**, 7233.
9   L. Noel-Duchesneau, N. Lugan, G. Lavigne, A. Labande and V. Ceśar, *Organometallics*, 2014, **33**, 5085.
10 H. Tinnermann, C. Wille and M. Alcarazo, *Angew. Chem., Int. Ed.*, 2014, **53**, 8732.
11 A. Feyrer and F. Breher, *Inorg. Chem. Front.*, 2017, **4**, 1125.
12 Selected examples: (a) I. M. Lorkovic, R. R. Duff and M. S. Wrighton, *J. Am. Chem. Soc.*, 1995, **117**, 3617; (b) C. K. A. Gregson, V. C. Gibson, N. J. Long, E. L. Marshall, P. J. Oxford and A. J. P. White, *J. Am. Chem. Soc.*, 2006, **128**, 7410; (c) X. Wang, A. Thevenon, J. L. Brosmer, I. Yu, S. I. Khan, P. Mehrkhodavandi and P. L. Diaconescu, *J. Am. Chem. Soc.*, 2014, **136**, 11264.
13 (a) A. Feyrer, M. K. Armbruster, K. Fink and F. Breher, *Chem. – Eur. J.*, 2017, **23**, 7402; (b) F. Walz, E. Moos, D. Garnier, R. Köppe, C. E. Anson and F. Breher, *Chem. – Eur. J.*, 2017, **23**, 1173.
14 (a) A. M. Allgeier and C. A. Mirkin, *Angew. Chem., Int. Ed.*, 1998, **37**, 894; (b) V. Blanco, D. A. Leigh and V. Marcos, *Chem. Soc. Rev.*, 2015, **44**, 5341; (c) O. R. Luca and C. H. Crabtree, *Chem. Soc. Rev.*, 2013, **42**, 1440.
15 Selected recent reviews: (a) A. M. Asiri and A. S. K. Hashmi, *Chem. Soc. Rev.*, 2016, **45**, 4471; (b) A. Fürstner, *Angew. Chem., Int. Ed.*, 2018, **57**, 4215; (c) R. Dorel and A. M. Echavarren, *Chem. Rev.*, 2015, **115**, 9028; (d) A. S. K. Hashmi, *Angew. Chem., Int. Ed.*, 2010, **49**, 5232.
16 (a) L. Huang, M. Arndt, K. Gooßen, H. Heydt and L. J. Gooßen, *Chem. Rev.*, 2015, **115**, 2596; (b) R. A. Widenhoefer and X. Han, *Eur. J. Org. Chem.*, 2006, 4555.
17 W. Wang, G. B. Hammond and B. Xu, *J. Am. Chem. Soc.*, 2012, **134**, 5697.
18 D. Malhotra, M. S. Mashuta, G. B. Hammond and B. Xu, *Angew. Chem., Int. Ed.*, 2014, **53**, 4456.
19 C. A. Gaggioli, G. Ciancaleoni, D. Zuccaccia, G. Bistoni, L. Belpassi, F. Tarantelli and P. Belanzoni, *Organometallics*, 2016, **35**, 2275.
20 (a) T. Witteler, H. Darmandeh, P. Mehlmann and F. Dielmann, *Organometallics*, 2018, **37**, 3064; (b) Footnote 33 of ref. 3.
21 (a) S. González-Gallardo, I. Kuzu, P. Oña-Burgos, T. Wolfer, C. Wang, K. W. Klinkhammer, W. Klopper, S. Bräse and F. Breher, *Organometallics*, 2014, **33**, 941; (b) J. M. Serrano-Becerra, A. F. G. Maier, S. González-Gallardo, E. Moos, C. Kaub, M. Gaffga, G. Niedner-Schatteburg, P. W. Roesky, F. Breher and J. Paradies, *Eur. J. Org. Chem.*, 2014, 4515.
22 (a) M. Herberhold and H.-D. Brendel, *J. Organomet. Chem.*, 1993, **458**, 205; (b) M. Herberhold, A. Hofmann and W. Milius, *J. Organomet. Chem.*, 1998, **555**, 187.
23 (a) P. Pérez-Galán, N. Delpont, E. Herrero-Gómez, F. Maseras and A. M. Echavarren, *Chem. – Eur. J.*, 2010, **16**, 5324; (b) A. S. K. Hashmi, B. Bechem, A. Loos, M. Hamzic, F. Rominger and H. Rabaa, *Aust. J. Chem.*, 2014, **67**, 481; (c) J. T. Fleming, P. G. Waddell, M. R. Probert, W. Clegg and L. J. Higham, *Eur. J. Inorg. Chem.*, 2017, 2837.
24 L. Falivene, R. Credendino, A. Poater, A. Petta, L. Serra, R. Oliva, V. Scarano and L. Cavallo, *Organometallics*, 2016, **35**, 2286.
25 E. Deck and F. Breher, unpublished results.
26 A. R. Chianese, X. Li, M. C. Janzen, J. W. Faller and R. H. Crabtree, *Organometallics*, 2003, **22**, 1663.
27 C. D. Varnado, Jr., E. L. Rosen, M. S. Collins, V. M. Lynch and C. W. Bielawski, *Dalton Trans.*, 2013, **42**, 13251.
28 (a) L. Hettmanczyk, S. Manck, C. Hoyer, S. Hohloch and B. Sarkar, *Chem. Commun.*, 2015, **51**, 10949; (b) L. Hettmanczyk, L. Suntrup, S. Klenk, C. Hoyer and B. Sarkar, *Chem. – Eur. J.*, 2017, **23**, 576; (c) S. Klenk, S. Rupf, L. Suntrup, M. van der Meer and B. Sarkar, *Organometallics*, 2017, **36**, 2026.
29 (a) S. Ibáñez, M. Poyatos, L. N. Dawe, D. Gusev and E. Peris, *Organometallics*, 2016, **35**, 2747; (b) P. Veit, C. Volkert, C. Förster, V. Ksenofontov, S. Schlicher, M. Bauer and K. Heinze, *Chem. Commun.*, 2019, DOI: 10.1039/c9cc00283a.
30 All attempts to prepare the cationic complexes, *e.g.* **4⁺**, on a preparative scale have not yet been successful.
31 E. Mizushima, T. Hayashi and M. Tanaka, *Org. Lett.*, 2003, **5**, 3349.
32 V. Lavallo, J. H. Wright, F. S. Tham and S. Quinlivan, *Angew. Chem., Int. Ed.*, 2013, **52**, 3172.